

1 **Title: Evidence for the coupling of substrate recognition with transporter opening in**

2 **MOP-family flippases**

3 **Authors:** Lok To Sham<sup>1,3</sup>, Sanduo Zheng<sup>2</sup>, Andrew C. Kruse<sup>2</sup>, and Thomas G. Bernhardt<sup>1\*</sup>

4 **Affiliations:**

5 <sup>1</sup>Department of Microbiology and Immunobiology  
6 Harvard Medical School  
7 Boston, MA 02115

8  
9 <sup>2</sup>Department of Biological Chemistry and Molecular Pharmacology  
10 Harvard Medical School  
11 Boston, MA 02115

12  
13 <sup>3</sup>Department of Microbiology and Immunology  
14 National University of Singapore  
15 Singapore, 117545

16  
17  
18 \*To whom correspondence should be addressed.  
19 Thomas G. Bernhardt, Ph.D.  
20 Harvard Medical School  
21 Department of Microbiology and Immunobiology  
22 Boston, Massachusetts 02115  
23 e-mail: [thomas\\_bernhardt@hms.harvard.edu](mailto:thomas_bernhardt@hms.harvard.edu)

24  
25  
26  
27 **Running title:** Flippase substrate specificity

28  
29 **Classification:** BIOLOGICAL SCIENCES; MICROBIOLOGY

30  
31 **Keywords:** peptidoglycan, cell wall, MurJ, flippase, MOP-family transporters

32 **ABSTRACT**

33 Bacteria produce a variety of surface-exposed polysaccharides important for cell integrity,  
34 biofilm formation, and evasion of the host immune response. Synthesis of these polymers  
35 often involves the assembly of monomer oligosaccharide units on the lipid carrier  
36 undecaprenyl-phosphate at the inner face of the cytoplasmic membrane. For many polymers,  
37 including cell wall peptidoglycan, the lipid-linked precursors must be transported across the  
38 membrane by flippases to facilitate polymerization at the membrane surface. Flippase activity  
39 for this class of polysaccharides is most often attributed to MOP (Multidrug/Oligosaccharidyl-  
40 lipid/Polysaccharide) family proteins. Little is known about how this ubiquitous class of  
41 transporters identifies and translocates its cognate precursor over the many different types of  
42 lipid-linked oligosaccharides produced by a given bacterial cell. To investigate the specificity  
43 determinants of MOP proteins, we selected for variants of the WzxC flippase involved in  
44 *Escherichia coli* capsule (colanic acid) synthesis that can substitute for the essential MurJ  
45 MOP-family protein and promote transport of cell wall peptidoglycan precursors. Variants with  
46 substitutions predicted to destabilize the inward-open conformation of WzxC lost substrate  
47 specificity and supported both capsule and peptidoglycan synthesis. Our results thus suggest  
48 that specific substrate recognition by a MOP transporter normally destabilizes the inward-open  
49 state, promoting transition to the outward-open conformation and concomitant substrate  
50 translocation. Furthermore, the ability of WzxC variants to suppress MurJ inactivation provides  
51 strong support for the designation of MurJ as the flippase for peptidoglycan precursors, the  
52 identity of which has been controversial.

53

54 **SIGNIFICANCE**

55 From cell walls in bacteria to protein glycosylation in eukaryotes, surface exposed  
56 polysaccharides are built on polyprenol-phosphate lipid carriers. Monomer units are typically  
57 assembled at the cytoplasmic face of the membrane and require translocation to the cell  
58 surface for polymerization/assembly. MOP-family proteins are a major class of transporters  
59 associated with this flippase activity. Despite their ubiquity and importance for cell surface  
60 biology, little is known about their transport mechanism. Here, we investigated substrate  
61 recognition by MOP transporters in bacteria. We present evidence that transport proceeds via  
62 destabilization of the inward-open state of the transporter by specific substrate binding thereby  
63 promoting a transition to the outward-open state and substrate release on the opposite face of  
64 the membrane.

65

66 **body**

67 **INTRODUCTION**

68 Bacterial cells produce a variety of cell surface polysaccharides. Polymers like peptidoglycan  
69 (PG) and teichoic acids (TAs) are critical for cell integrity and shape maintenance, whereas  
70 capsular polysaccharides and O-antigens play central roles in virulence and the evasion of  
71 host defenses (1). Despite their vast structural diversity, the majority of surface  
72 polysaccharides are made by one of three types of synthesis and export mechanisms:  
73 synthase-dependent, ABC transporter-dependent, or Wzy-dependent pathways (1). Most  
74 complex polysaccharides with 3-6 sugars in their repeating unit are made by the widely-  
75 distributed Wzy-dependent pathway (2). Examples include O-antigens of gram-negative  
76 bacteria and many capsular polysaccharides. For these polymers, the monomeric  
77 oligosaccharide unit is synthesized at the inner face of the cytoplasmic membrane on the lipid  
78 carrier undecaprenyl phosphate (Und-P) (2, 3). For polymerization, the oligosaccharide moiety  
79 must be transported across the membrane and exposed at the membrane surface by a class  
80 of transporters referred to as flippases (3, 4). Notably, this overall lipid-linked synthesis  
81 strategy is near universal as it is also employed by eukaryotic cells to generate  
82 oligosaccharides for N-linked protein glycosylation (5).

83

84 Lipid-linked sugar flippase activity for polysaccharide synthesis has principally been ascribed  
85 to one of two types of transporters: ABC (ATP-binding cassette) systems, and MOP  
86 (Multidrug/Oligosaccharidyl-lipid/Polysaccharide) family proteins (3). MOP-type flippases are  
87 typically associated with Wzy-dependent polysaccharide synthesis pathways, and several lines  
88 of evidence indicate that they have a strong preference for translocating the specific lipid-  
89 linked oligosaccharide produced by their cognate synthetic pathway (6-8). How these

90 transporters specifically recognize their substrates over the many different types of lipid-linked  
91 oligosaccharides produced in a bacterial cell is not currently known. The transport mechanism  
92 is also poorly understood, but the recently solved structures of the MOP-family protein MurJ  
93 from *Thermosipho africanus* and *Escherichia coli* has provided important clues (9, 10).

94

95 MurJ was identified several years ago as a protein essential for PG biogenesis. It was  
96 proposed to be the long-sought after flippase that translocates the final PG precursor lipid II  
97 (11, 12), which consists of the disaccharide N-acetylmuramic acid (MurNAc)- $\beta$ -1-4-N-  
98 acetylglucosamine (GlcNAc) with a pentapeptide attached to the MurNAc sugar via a lactyl  
99 group. Like other polysaccharide synthesis pathways, lipid II is assembled on the inner face of  
100 the cytoplasmic membrane and must be translocated before it can be polymerized and  
101 crosslinked to form the PG matrix that fortifies bacterial cells against osmotic rupture (3).  
102 Importantly, the functional assignment of MurJ as the PG lipid II flippase remains controversial  
103 in the field of PG biogenesis because in vitro assays have detected what appears to be lipid II  
104 flippase activity for the SEDS (shape, elongation, division, sporulation) family protein FtsW (3,  
105 13).

106

107 In support of a flippase function for MurJ, it was found to be required for lipid II translocation in  
108 *Escherichia coli* using an *in vivo* flippase assay whereas SEDS proteins were dispensable for  
109 this activity (12). The structure of MurJ from *T. africanus* also supports a transporter function  
110 (9). In the crystals, the protein adopted an inward-open conformation with a solvent accessible  
111 cavity capable of accommodating the lipid II head group. Related structures of a different  
112 subfamily of MOP transporters involved in drug efflux had previously been solved in an  
113 outward-open conformation (14), and chemical probing of MurJ structure in vivo (15) indicates

114 that MurJ can adopt such a conformation in cells. Evolutionary coupling (EC) analysis (16) also  
115 shows that MurJ must adopt an additional conformation not accounted for in the inward-open  
116 crystal structure, since pairs of distant residues on the cytosolic face so strong co-evolution. An  
117 outward-open model of MurJ similarly leaves predicted interactions unsatisfied on the  
118 periplasmic face of the protein, indicating that at least two distinct conformations are subject to  
119 evolutionary selective pressure (10). Thus, it has been proposed that MurJ and other MOPS  
120 family proteins mediate transport/flipping via an alternating access model involving the  
121 interconversion between the inward- and outward-facing conformations, alternately allowing  
122 the lipid II headgroup to access the cytosolic and periplasmic faces of the membrane (2, 3, 9,  
123 10).

124

125 To investigate the specificity determinants of MOP proteins, we selected for variants of the  
126 WzxC flippase involved in *Escherichia coli* capsule (colanic acid) synthesis (17) that gain  
127 translocation activity for peptidoglycan precursors and can substitute for the essential MurJ  
128 MOP-family protein in the cell wall synthesis pathway. Variants with amino acid changes  
129 predicted to destabilize the inward-open conformation of WzxC lost substrate specificity and  
130 supported both capsule and peptidoglycan synthesis. Our results thus suggest that specific  
131 substrate recognition by a MOP transporter normally functions to destabilize the inward-open  
132 state, promoting transition to the outward-open conformation and concomitant substrate  
133 translocation. Furthermore, the ability of WzxC variants to suppress MurJ inactivation provides  
134 strong support for the designation of MurJ as the flippase for peptidoglycan precursors.

135 **RESULTS**

136 **Identification of WzxC variants that can substitute for MurJ**

137 WzxC is a MOP-family transporter in *E. coli* required for the synthesis of the colanic acid  
138 capsule (17), the production of which is induced by activation of the Rcs envelope stress  
139 response (18). The colanic acid precursor is a hexasaccharide [L-fucose-(pyruyl-D-galactose-  
140 D-glucouronic acid-D-galactose)-O-acetyl-L-fucose-D-glucose] built on the Und-P lipid carrier.  
141 WzxC has been implicated in the transport (flipping) of this lipid-linked intermediate (17).  
142 Although WzxC is the closest relative of MurJ in *E. coli* ( $\approx 12\%$  sequence identity), its substrate  
143 structure differs greatly from the lipid II PG precursor that MurJ has been implicated in flipping.  
144 It is therefore not surprising that WzxC fails to substitute for MurJ and promote growth when  
145 MurJ is depleted (**Fig. 1, row 1**). However, we thought it might be possible to identify altered  
146 WzxC proteins that gain the ability to flip the PG precursor and rescue a MurJ defect. We  
147 reasoned that the isolation and characterization of such variants would provide useful  
148 information about what determines substrate specificity in MOP-family flippases and potentially  
149 reveal new insights into the transport mechanism.

150

151 To select for altered substrate specificity variants of WzxC, the *wzxC* gene was mutagenized  
152 using error-prone PCR and cloned into a medium copy vector under control of the lactose  
153 promoter ( $P_{lac}$ ). The resulting plasmid library was transformed into a MurJ-depletion strain  
154 where native *murJ* was engineered to be under control of the arabinose promoter ( $P_{ara}$ ). This  
155 promoter replacement renders the strain dependent on the presence of arabinose in the  
156 medium for growth. When the depletion strain harboring the *wzxC* plasmid library was plated  
157 on LB medium lacking arabinose but supplemented with isopropyl- $\beta$ -D-thiogalactopyranoside  
158 (IPTG) to induce *wzxC*, surviving colonies arose at a low frequency ( $10^{-4}$ ). To distinguish

159 between survivors with mutations allowing arabinose-independent expression of *murJ* from the  
160 desired *wzxC* mutants capable of substituting for *murJ*, plasmids were purified from the  
161 isolates and transformed back into the parental MurJ-depletion strain. The resulting  
162 transformants were then tested for growth on IPTG-containing medium with or without  
163 arabinose supplementation. Plasmids conferring arabinose-independent growth were then  
164 isolated and their *wzxC* insert was sequenced. Many of the primary isolates harbored *wzxC*  
165 clones with multiple mutations (**SI Appendix, Table S1**). To identify the functionally relevant  
166 substitutions, we used site-directed mutagenesis to construct plasmids encoding C-terminal  
167 FLAG-tagged WzxC variants (WzxC-FLAG) with single amino acid changes corresponding to  
168 those identified in the original mutant isolates. The FLAG-tag did not appear to interfere with  
169 WzxC activity as the fusion was capable of supporting capsule production in a  $\Delta wzxC$  strain  
170 (**SI Appendix, Fig. S1**). Importantly, wild-type WzxC-FLAG also failed to promote growth upon  
171 MurJ depletion (**Fig. 1, row 1**). In total, eleven single amino acid substitutions in WzxC-FLAG  
172 representing changes throughout the length of the 492 amino acid protein were found to be  
173 sufficient for suppression of MurJ depletion (**Fig. 1, rows 2-11**). The *wzxC* alleles varied in the  
174 strength of the observed suppression phenotype, with most being able to promote growth of  
175 the MurJ depletion strain upon induction with 25  $\mu$ M IPTG, but two requiring 75-100  $\mu$ M IPTG  
176 to achieve full suppression (**Fig. 1, rows 2-11, SI Appendix, Fig. S2**). Immunoblot analysis  
177 using anti-FLAG antibodies indicated that all of the WzxC-FLAG variants were produced at  
178 levels comparable to, or slightly lower than, the wild-type protein (**SI Appendix, Fig. S3**). Thus,  
179 the WzxC variants do not gain the ability to substitute for MurJ simply due to their  
180 overproduction.

181



182 To determine if the altered WzxC proteins could fully substitute for MurJ, we assessed the  
183 ability of eight variants for their ability to support the growth of a *murJ* deletion. A  $\Delta murJ::Kan^R$   
184 allele constructed in a background with a complementing *murJ* plasmid was used as a donor  
185 for P1 phage transduction of the deletion into MurJ<sup>+</sup> strains harboring the *wzxC* plasmids. For  
186 all the mutants tested, transductants were successfully isolated on medium containing IPTG  
187 for *wzxC* induction, and deletion/replacement of the native *murJ* gene was confirmed in each  
188 case (**SI Appendix, Fig. S4**). We conclude that many of the WzxC variants identified in the  
189 selection are capable of overcoming the complete loss of MurJ function. Therefore, we will  
190 henceforth refer to them as <sup>MJ</sup>WzxC derivatives.

191  
192 **<sup>MJ</sup>WzxC variants can support PG lipid II flipping in vivo**

193 The ability of the <sup>MJ</sup>WzxC variants to suppress the essentiality of MurJ suggests that they have  
194 gained the ability to transport the lipid II precursor for PG biogenesis. To test this possibility,  
195 we took advantage of an in vivo assay for lipid II flipping (12). To detect lipid II transport, cells  
196 were radiolabeled with the PG precursor [<sup>3</sup>H]-meso-diaminopimelic acid (mDAP) and treated  
197 with Colicin M (CoIM). This toxin invades the periplasm and cleaves flipped lipid II, generating  
198 a soluble pyrophospho-disaccharide pentapeptide that is subsequently converted to  
199 disaccharide tetrapeptide by periplasmic carboxypeptidases. When MurJ is functional, CoIM  
200 cleavage of flipped lipid II generates a new soluble radiolabeled product and destroys the  
201 labeled lipid fraction (12, 19) (**Fig. 2**). The MurJ variant, MurJ(A29C), is sensitive to the Cys-  
202 modifying reagent (2-sulfonatoethyl)methanethiosulfanate (MTSES). When radiolabeled cells  
203 relying on this MurJ derivative for lipid II translocation are treated with MTSES, the lipid fraction  
204 is protected from CoIM cleavage and the soluble CoIM product is not observed (12) (**Fig. 2**),  
205 indicating that flipping is blocked. A plasmid producing WzxC(WT) did not alleviate this block

206 **(Fig. 2)**. However, production of WzxC(V252M) restored lipid II cleavage by ColM in MurJ-  
207 inactivated cells and promoted the accumulation of the soluble ColM product **(Fig. 2)**. We  
208 therefore conclude that the <sup>MJ</sup>WzxC derivatives have gained the ability to facilitate lipid II  
209 transport.

210

### 211 **Most <sup>MJ</sup>WzxC derivatives have lost substrate specificity**

212 We next investigated whether the <sup>MJ</sup>WzxC variants that support lipid II translocation retain the  
213 ability to promote colanic acid capsule synthesis. Production of the capsule is induced by the  
214 Rcs stress response system when cells are grown in high-salt medium (20). Cells unable to  
215 make capsule grew poorly on LB medium containing 1.0 M NaCl **(Fig. 3A, row 1, SI**  
216 **Appendix, Fig. S1)**. This growth defect was observed for mutants blocked at the first step in  
217 the pathway ( $\Delta wcaJ$ ) or at the WzxC step. Thus, the phenotype does not require the build up  
218 of lipid-linked colanic acid precursors that would likely reduce the pool of lipid carrier available  
219 to other pathways like PG synthesis (21). Production of wild-type WzxC-FLAG as well as most  
220 of the <sup>MJ</sup>WzxC-FLAG derivatives restored the growth of  $\Delta wzxC$  cells on LB with 1.0M NaCl  
221 **(Fig. 3A, rows 2-13)**. The exception was WzxC(T159K), which suppressed MurJ depletion, but  
222 not the  $\Delta wzxC$  phenotype. Thus, the majority of the <sup>MJ</sup>WzxC proteins appear to retain WzxC  
223 function.

224

225 To further investigate the range of potential substrates capable of being utilized by the <sup>MJ</sup>WzxC  
226 variants, we tested their ability to participate in O-antigen synthesis. These polysaccharides  
227 decorate the lipopolysaccharides (LPS) that form the outer leaflet of the outer membrane in  
228 gram-negative bacteria (22). *E. coli* K-12 strains, including the MG1655 derivatives used here,  
229 do not make O-antigen polymers. This defect is due to an insertion element that disrupts *wbbL*,

230 which encodes the enzyme catalyzing the committed step for the synthesis of the O-16 antigen  
231 with the repeating unit D-galactose-D-glucose-L-rhamnose-(D-glucose)-D-N-  
232 acetylglucosamine (23). The flippase for this pathway is thought to be WzxB (24). Inactivation  
233 of *wzxB* is not lethal in *WbbL*<sup>-</sup> strains. However, ectopic expression of *wbbL* in  $\Delta$ *wzxB* cells is  
234 lethal, presumably due to the accumulation of lipid-linked O-16 precursors and the  
235 sequestration of Und-P lipid carrier from the PG synthesis pathway (21, 25). Unlike wild-type  
236 WzxC-FLAG, co-production of many of the <sup>MJ</sup>WzxC-FLAG variants with *WbbL* rescued the  
237 *WbbL*-induced lethality of  $\Delta$ *wzxB* cells and restore O-antigen production (**Fig. 3B, SI**  
238 **Appendix, Fig. S5**). However, two variants, WzxC(P262R) and WzxC(T384M) that  
239 complemented the MurJ-depletion and  $\Delta$ *wzxC* phenotypes failed substitute for WzxB. On the  
240 other hand, WzxC(T159K), which failed to complement  $\Delta$ *wzxC* rescued both the  $\Delta$ *wzxB* and  
241 MurJ-depletion phenotypes. From these results, we conclude that the <sup>MJ</sup>WzxC variants have  
242 largely lost substrate specificity, allowing them to function in a variety of polysaccharide  
243 synthesis pathways.

244

### 245 **Substitutions in the <sup>MJ</sup>WzxC variants are predicted to destabilize the inward-open** 246 **conformation**

247 In order to better understand the molecular basis for the effects of the <sup>MJ</sup>WzxC mutations, we  
248 constructed a homology model of WzxC using the crystal structure of *E. coli* MurJ (10) as a  
249 template (**Fig. 4, SI Appendix, Fig. S5**). We expected that most of the specificity altering  
250 changes in WzxC would occur in the aqueous cavity of the transporter where substrate is  
251 predicted to bind. However, when mapped onto the model WzxC structure, the majority of  
252 residues altered in the <sup>MJ</sup>WzxC variants clustered at or near the periplasmic face of the protein.  
253 Many of these substitutions occur in residues that mediate inter-domain contact between the

254 N-lobe and C-lobe on the periplasmic side (A33, A243, F41 and W320). For example, the  
255 pseudo-symmetry related pair of residues A33 and A243 are in small, sterically restricted  
256 spaces (**SI Appendix, Fig. S5A**). Mutation of these to Val or Thr is incompatible with the  
257 inward-open homology model due to steric clash with neighboring residues, and so is expected  
258 to destabilize the inward-open conformation. Similarly, the buried N-lobe residue F41 engages  
259 in extensive hydrophobic contacts with L248, F316, and other residues in the C-lobe, so its  
260 mutagenic substitution with Leu may destabilize the inward-open conformation (**SI Appendix,**  
261 **Fig. S5A**). Likewise, W320 sits near the interface between the two lobes, and the  
262 nonconservative substitution with Arg likely weakens interdomain interactions on the  
263 periplasmic side (**SI Appendix, Fig. S5A**). It is noteworthy that most of these substitutions are  
264 modest. They may simply raise the energy of the inward-open state, altering the equilibrium  
265 between inward-open and outward-open states without causing a complete loss of function.  
266  
267 Other substitutions are not located at the interdomain interface but rather are found in or near  
268 the central cavity of the enzyme. For instance, P262 and V252 sit in the lateral gate between  
269 TM1 and TM8 (**SI Appendix, Fig. S5B**). Both residues may be directly involved in substrate  
270 binding or play a critical role in conformation transition. Their alteration may expand the range  
271 of substrates accepted by transporter by affecting substrate binding affinity. Notably, L429 is  
272 located neither in the central cavity nor in the extracellular gate, but rather is found in TM13 (**SI**  
273 **Appendix, Fig. S5C**). Its mutation to proline is incompatible with  $\alpha$ -helical geometry, and must  
274 force a distortion in the helix. The connection between this effect and broadened substrate  
275 specificity is unclear, but attests to a functionally important role for TMs 13 and 14, which are  
276 absent in most MOP family flippases.

277 **DISCUSSION**

278 In this report, we isolated <sup>MJ</sup>WzxC variants that have lost substrate specificity and gain the  
279 ability to transport the PG precursor lipid II and O-antigen precursors in addition to its native  
280 substrate for colanic acid synthesis. The location of the amino acid changes in WzxC resulting  
281 in this phenotype was surprising. Rather than altering the predicted substrate-binding region of  
282 the modeled structure, the changes largely map to portions of the protein located near the  
283 periplasmic face of the membrane. Based on the MurJ structure, this region of the protein is  
284 predicted to form contacts that stabilize the inward-open conformation of the transporter.  
285 Because many of the amino acid substitutions in the <sup>MJ</sup>WzxC variants involve a change in side  
286 chain size or charge, we infer that they exert their effect on the transporter through the  
287 destabilization of the inward-open conformation. Thus, the genetic results support a model in  
288 which the stability of the inward-open conformation plays a key role in determining the  
289 substrate specificity of the transporter (**Fig. 5**).

290  
291 We propose that for wild-type WzxC, a specific interaction between the native substrate and  
292 the hydrophilic core of the transporter is needed to break contacts at the periplasmic face of  
293 the membrane involved in stabilizing the inward-open conformation. Such a change would then  
294 facilitate the transition to the outward-open conformation and the release of substrate on the  
295 outside face of the membrane. Once substrate is released, the protein would then be free to  
296 transition back to the more stable inward-open conformation and begin another round of  
297 transport. Due to the changes in the <sup>MJ</sup>WzxC variants, we envision that the protein can more  
298 readily interconvert between the two main conformations without the need for specific  
299 substrate binding. Thus, the transport of non-native precursors would be facilitated by the  
300 altered flippase. The main limitation in this case is likely to be the ability of the precursor sugar

301 moiety to fit within the hydrophilic core of the altered transporter. WzxC was therefore an  
302 especially fortuitous choice for this specificity study. Its native substrate is relatively large such  
303 that the hydrophilic core of the <sup>MJ</sup>WzxC variants is likely capable of accommodating and  
304 flipping a wider range of substrates than might be possible with other transporters.

305

306 The phenotype of a previously isolated mutant in a different flippase suggests that other  
307 transporters may function similarly to WzxC. TacF is a MOP family protein implicated in the  
308 transport of teichoic acid (TA) precursors of *Streptococcus pneumoniae* (26). The LTAs in this  
309 organisms are normally decorated with choline (27). A TacF variant was identified that  
310 suppressed the choline-dependent growth phenotype of *S. pneumoniae*, presumably by  
311 allowing the transport of LTA precursors lacking choline (26). The change in this variant that  
312 alters the substrate choline requirement is located in a loop of TacF predicted to be at the  
313 outer surface of the membrane (26). Similar to WzxC, this area is exactly where contacts that  
314 stabilize the inward-open conformation are likely to be made. Thus, the use of a specific  
315 substrate binding event to destabilize the inward-open state and promote a conformational  
316 transition may be a general component of the transport mechanism of MOP family flippases.  
317 Substrate-induced conformational changes have also been implicated in the transport  
318 mechanism of the (NSS) family of transporters (28), suggesting that they may be involved in  
319 many different types of membrane transport processes.

320

321 In addition to a better understanding of the transport mechanism of MOP family flippases, the  
322 activities of the <sup>MJ</sup>WzxC variants also provide insight into the process of PG biogenesis.  
323 Although flippase activity has yet to be demonstrated for MurJ in vitro, the finding that a protein  
324 implicated in flipping colanic acid precursors can substitute for MurJ in PG biogenesis makes it

325 hard to argue that MurJ is anything other than the lipid II flippase. Furthermore, the ability of  
326 <sup>MJ</sup>WzxC variants as well as other heterologous or promiscuous flippase proteins to maintain  
327 growth and viability upon MurJ inactivation suggests that lipid II transport does not need to  
328 occur in the context of specific multi-protein complexes with other PG biogenesis factors. Such  
329 complexes may be formed to render the process more efficient, but they do not appear to be  
330 necessary for the construction of the PG layer.

331

332 In conclusion, our results highlight the utility of unbiased genetic selections to study the  
333 function of MOP family flippases. Further structural analysis of these transporters using the  
334 substitutions identified in the <sup>MJ</sup>WzxC variants should facilitate the capture of additional  
335 conformations of these proteins and provide further insight into their transport mechanism.

336

## 337 **MATERIALS AND METHODS**

### 338 **Media, Bacterial Strains and Plasmids**

339 Strains used in this study are listed in **SI Appendix, Table S2**. Unless otherwise specified, *E.*  
340 *coli* cells were grown in lysogeny broth (LB) under aeration at 37°C. Where indicated,  
341 arabinose and glucose are added to a final concentrations of 0.2% (w/v). The antibiotics  
342 ampicillin, chloramphenicol, and kanamycin were used at a final concentration of 25 µg/ml.  
343 Spectinomycin was added to a final concentration of 40 µg/ml. Plasmids and oligonucleotides  
344 used in this study are listed in **SI Appendix, Table S3 and S4**, respectively.

### 345 346 **Selection of WzxC variants that can suppress MurJ essentiality**

347 Strain CS7 [ $P_{ara}::murJ$ ] was transformed with a mutagenized *wzxC* plasmid library ( $P_{lac}::wzxC$ )  
348 (see **SI appendix** for details). Transformants were scraped from the agar surface into 5ml of  
349 LB medium and the resulting cell suspension was serially diluted and plated on LB agar  
350 supplemented with chloramphenicol, 0.2% glucose, and IPTG. Isolates that required induction  
351 of the *wzxC* plasmid with IPTG for growth in the absence of *murJ* expression (0.2% glucose)  
352 were selected for sequencing.

### 353 354 **Detection of lipid II flippase activity using Colicin M**

355 Lipid II translocation across the inner membrane was monitored using the previously described  
356 colicin M assay (12). Cells of CAM290/pCS124 [ $murJ(A29C)/P_{lac}::wzxC$ ] and CAM290/pDF2  
357 [ $murJ(A29C)/P_{lac}::wzxC(V252M)$ ] were grown in LB medium with chloramphenicol overnight.  
358 Cultures were diluted 100 fold in 40ml of the labeling medium with 100µM IPTG (M9  
359 supplemented with 0.1% (w/v) casamino acids, 0.2% (w/v) maltose, 0.1mg/ml of lysine,  
360 threonine and methionine) and grown at 37°C with aeration. When the culture  $OD_{600}$  reached



361 0.2, 15 $\mu$ l of 1.5  $\mu$ Ci/ $\mu$ l of  $^3$ H-mDAP (ARC) was added to 10ml of the culture and incubated for  
362 15 minutes at 37°C. When indicated, colicin M and MTSES were added to a final concentration  
363 of 500 ng/ml and 0.4 mM, respectively. The cultures were then incubated for 10 minutes and  
364 chilled immediately on ice. Cells were collected by centrifugation at 8,000 x *g* for 2 minutes at  
365 4°C and resuspended in 1ml of preheated water. Samples were then boiled for 30 minutes and  
366 processed to measure the soluble colicin M product and PG lipid precursors as described  
367 previously (12).

368

### 369 **Homology model construction**

370 A homology model of *E. coli* WzxC was constructed in MODELLER (29) using a multi-template  
371 modeling protocol with the crystal structures of MurJ from *E. coli* (10) and *T. africanus* (9)  
372 (PDB ID: 5T77) serving as templates.

373

374 **ACKNOWLEDGEMENTS**

375 The authors would like to thank all members of the Bernhardt, Rudner, and Kruse labs for  
376 helpful advice and discussions. This work was supported by the National Institutes of Health  
377 (R01AI083365 and AI099144 to TGB, and CETR U19 AI109764 to TGB and ACK).

378

379 **REFERENCES**

- 380 1. Whitfield C (2006) Biosynthesis and assembly of capsular polysaccharides in  
381 *Escherichia coli*. *Annu Rev Biochem* 75:39–68.
- 382 2. Islam ST, Lam JS (2014) Synthesis of bacterial polysaccharides via the Wzx/Wzy-  
383 dependent pathway. *Can J Microbiol* 60(11):697–716.
- 384 3. Ruiz N (2015) Lipid Flippases for Bacterial Peptidoglycan Biosynthesis. *Lipid Insights*  
385 8s1:LPI.S31783.
- 386 4. Islam ST, Lam JS (2013) Wzx flippase-mediated membrane translocation of sugar  
387 polymer precursors in bacteria. *Environ Microbiol* 15(4):1001–1015.
- 388 5. Helenius J, et al. (2002) Translocation of lipid-linked oligosaccharides across the ER  
389 membrane requires Rft1 protein. *Nature* 415(6870):447–450.
- 390 6. Liu MA, Stent TL, Hong Y, Reeves PR (2015) Inefficient translocation of a truncated O  
391 unit by a *Salmonella* Wzx affects both O-antigen production and cell growth. *FEMS*  
392 *Microbiol Lett* 362(9):725.
- 393 7. Hong Y, Reeves PR (2014) Diversity of o-antigen repeat unit structures can account for  
394 the substantial sequence variation of *wzx* translocases. *J Bacteriol* 196(9):1713–1722.
- 395 8. Hong Y, Liu MA, Reeves PR (2018) Progress in Our Understanding of Wzx Flippase for  
396 Translocation of Bacterial Membrane Lipid-Linked Oligosaccharide. *J Bacteriol*  
397 200(1):e00154–17.

- 398 9. Kuk ACY, Lee S-Y (2017) Crystal structure of the MOP flippase MurJ in an inward-  
399 facing conformation. *Nat Struct Mol Biol* 24(2):171–176.
- 400 10. Zheng S, et al. (2018) Structure and function of the lipid II flippase MurJ from  
401 *Escherichia coli*. *BioRxiv*
- 402 11. Ruiz N (2008) Bioinformatics identification of MurJ (MviN) as the peptidoglycan lipid II  
403 flippase in *Escherichia coli*. *Proc Natl Acad Sci USA* 105(40):15553–15557.
- 404 12. Sham L-T, et al. (2014) Bacterial cell wall. MurJ is the flippase of lipid-linked precursors  
405 for peptidoglycan biogenesis. *Science* 345(6193):220–222.
- 406 13. Mohammadi T, et al. (2011) Identification of FtsW as a transporter of lipid-linked cell  
407 wall precursors across the membrane. *EMBO J* 30(8):1425–1432.
- 408 14. He X, et al. (2010) Structure of a cation-bound multidrug and toxic compound extrusion  
409 transporter. *Nature* 467(7318):991–994.
- 410 15. Butler EK, Davis RM, Bari V, Nicholson PA, Ruiz N (2013) Structure-function analysis of  
411 MurJ reveals a solvent-exposed cavity containing residues essential for peptidoglycan  
412 biogenesis in *Escherichia coli*. 195(20):4639–4649.
- 413 16. Hopf TA, et al. (2014) Sequence co-evolution gives 3D contacts and structures of  
414 protein complexes. *elife* 3:65.
- 415 17. Stevenson G, Andrianopoulos K, Hobbs M, Reeves PR (1996) Organization of the  
416 *Escherichia coli* K-12 gene cluster responsible for production of the extracellular  
417 polysaccharide colanic acid. *J Bacteriol* 178(16):4885–4893.

- 418 18. Majdalani N, Gottesman S (2005) The Rcs phosphorelay: a complex signal transduction  
419 system. *Annu Rev Microbiol* 59:379–405.
- 420 19. Ghachi El M, et al. (2006) Colicin M exerts its bacteriolytic effect via enzymatic  
421 degradation of undecaprenyl phosphate-linked peptidoglycan precursors. *J Biol Chem*  
422 281(32):22761–22772.
- 423 20. Sledjeski DD, Gottesman S (1996) Osmotic shock induction of capsule synthesis in  
424 *Escherichia coli* K-12. *J Bacteriol* 178(4):1204–1206.
- 425 21. Jorgenson MA, Young KD (2016) Interrupting Biosynthesis of O Antigen or the  
426 Lipopolysaccharide Core Produces Morphological Defects in *Escherichia coli* by  
427 Sequestering Undecaprenyl Phosphate. *J Bacteriol* 198(22):3070–3079.
- 428 22. Raetz CRH, Reynolds CM, Trent MS, Bishop RE (2007) Lipid A modification systems in  
429 gram-negative bacteria. *Annu Rev Biochem* 76:295–329.
- 430 23. Liu D, Reeves PR (1994) *Escherichia coli* K12 regains its O antigen. *Microbiology*  
431 140(1):49–57.
- 432 24. Marolda CL (2004) Wzx proteins involved in biosynthesis of O antigen function in  
433 association with the first sugar of the O-specific lipopolysaccharide subunit.  
434 *Microbiology* 150(12):4095–4105.
- 435 25. Marolda CL, Tatar LD, Alaimo C, Aebi M, Valvano MA (2006) Interplay of the Wzx  
436 translocase and the corresponding polymerase and chain length regulator proteins in  
437 the translocation and periplasmic assembly of lipopolysaccharide O antigen. *J Bacteriol*  
438 188(14):5124–5135.

- 439 26. Damjanovic M, Kharat AS, Eberhardt A, Tomasz A, Vollmer W (2007) The Essential  
440 tacF Gene Is Responsible for the Choline-Dependent Growth Phenotype of  
441 *Streptococcus pneumoniae*. *J Bacteriol* 189(19):7105–7111.
- 442 27. Massidda O, Nováková L, Vollmer W (2013) From models to pathogens: how much  
443 have we learned about *Streptococcus pneumoniae* cell division? *Environ Microbiol*  
444 15(12):3133–3157.
- 445 28. Billesbølle CB, et al. (2015) Substrate-induced Unlocking of the Inner Gate Determines  
446 the Catalytic Efficiency of a Neurotransmitter:Sodium Symporter. *J Biol Chem*  
447 290(44):26725–26738.
- 448 29. Webb B, Sali A (2002) Comparative Protein Structure Modeling Using MODELLER.  
449 *Curr Protoc Bioinformatics* 235:5.6.1–5.6.32.

450 **FIGURE LEGENDS**

451 **Figure 1. WzxC variants can substitute for MurJ.** Cells of CS7 [ $P_{ara}::murJ$ ] harboring  
452 plasmids encoding C-terminally FLAG-tagged WzxC (WT) or the indicated derivatives were  
453 grown in LB medium with arabinose overnight. Following normalization for culture density,  
454 serial dilutions ( $10^{-1}$  to  $10^{-6}$ ) were prepared and 5  $\mu$ l of each were spotted onto LB plates  
455 supplemented with either glucose or IPTG. Plates were photographed after incubation at 37°C  
456 for  $\approx$ 16 hours. All of the strains grew similarly on plates supplemented with arabinose under  
457 this condition. An additional growth experiment with additional concentrations of IPTG are  
458 presented in **SI Appendix, Fig. S2.**

459

460 **Figure 2. Support of PG lipid-II flipping in vivo by a WzxC variant.** Cells of CAM290  
461 [ $murJ(A29C)$ ] harboring plasmid pCS124 [ $P_{lac}::wzxC(WT)-flag$ ] or pDF2 [ $P_{lac}::wzxC(V252M)-$   
462  $flag$ ] were grown in labeling medium to an OD<sub>600</sub> of 0.2. [<sup>3</sup>H]-mDAP was then added to  
463 radiolabel PG precursors. After a 15 min labeling period, MTSES and ColM were added to  
464 block MurJ(A29C) activity and cleave flipped lipid II, respectively. Just prior to cell lysis, cells  
465 were collected by centrifugation and fractionated to measure radioactivity in the PG lipid  
466 precursor pool (**A**) and soluble ColM cleavage product (**B**). WT and Mut denote WzxC(WT)  
467 and WzxC(V252M), respectively. The means and the standard error of means (SEMs) from  
468 three experiments are shown. P-values were calculated with two-tailed unpaired Student's t-  
469 test. \*,  $p < 0.05$ ; \*\*,  $p < 0.01$ ; n.s., not significant. cpm = counts per minute.

470

471 **Figure 3. Transport of colanic acid and O-antigen precursors by <sup>MJ</sup>WzxC variants. (A)**  
472 Cells of CS38 [ $\Delta wzxC$ ] harboring an empty vector (vector) or vectors encoding the indicated  
473 FLAG-tagged WzxC variant were grown and plated on LB medium with 1M NaCl as described

474 in Figure 1. Complementation of the  $\Delta wzxC$  phenotype results in the formation of mucoid  
475 colonies on the high-salt medium. **(B)** Cells of CS39/pCS160 [ $\Delta wzxB/P_{ara}::wbbL$ ] harboring the  
476 same WzxC-encoding plasmids were grown and diluted as described in Figure 1 followed by  
477 plating on LB medium with 100  $\mu$ M IPTG (to induce WzxC production) plus either glucose or  
478 arabinose (to repress or induce O-antigen production, respectively) as indicated.

479

#### 480 **Figure 4. Structural analysis of specificity-broadening mutations in WzxC.**

481 A homology model of WzxC is shown, with the sites of mutations highlighted in orange sticks.  
482 At left, the protein is viewed from the periplasmic side, and at right is viewed parallel to the  
483 membrane plane. With only a few exceptions, the mutations cluster at the periplasmic face of  
484 the protein near the interface between the N- and C-terminal lobes of WzxC.

485

486

#### 487 **Figure 5. Model for substrate induced conformational changes in MOP family flippases.**

488 Shown is a schematic summarizing our model for substrate transport by MOP family flippases.  
489 Structural studies suggest that the inward-open conformation is the most stable state of the  
490 transporter. Based on our genetic results, we propose that specific substrate binding is  
491 required to break contacts at the outer face of the transporter to destabilize the inward-open  
492 conformation. Once these contacts are broken, a transition to the outward-open conformation  
493 can occur to allow for substrate release on the opposite face of the membrane. For simplicity,  
494 the lipid anchor of the substrate is not drawn.



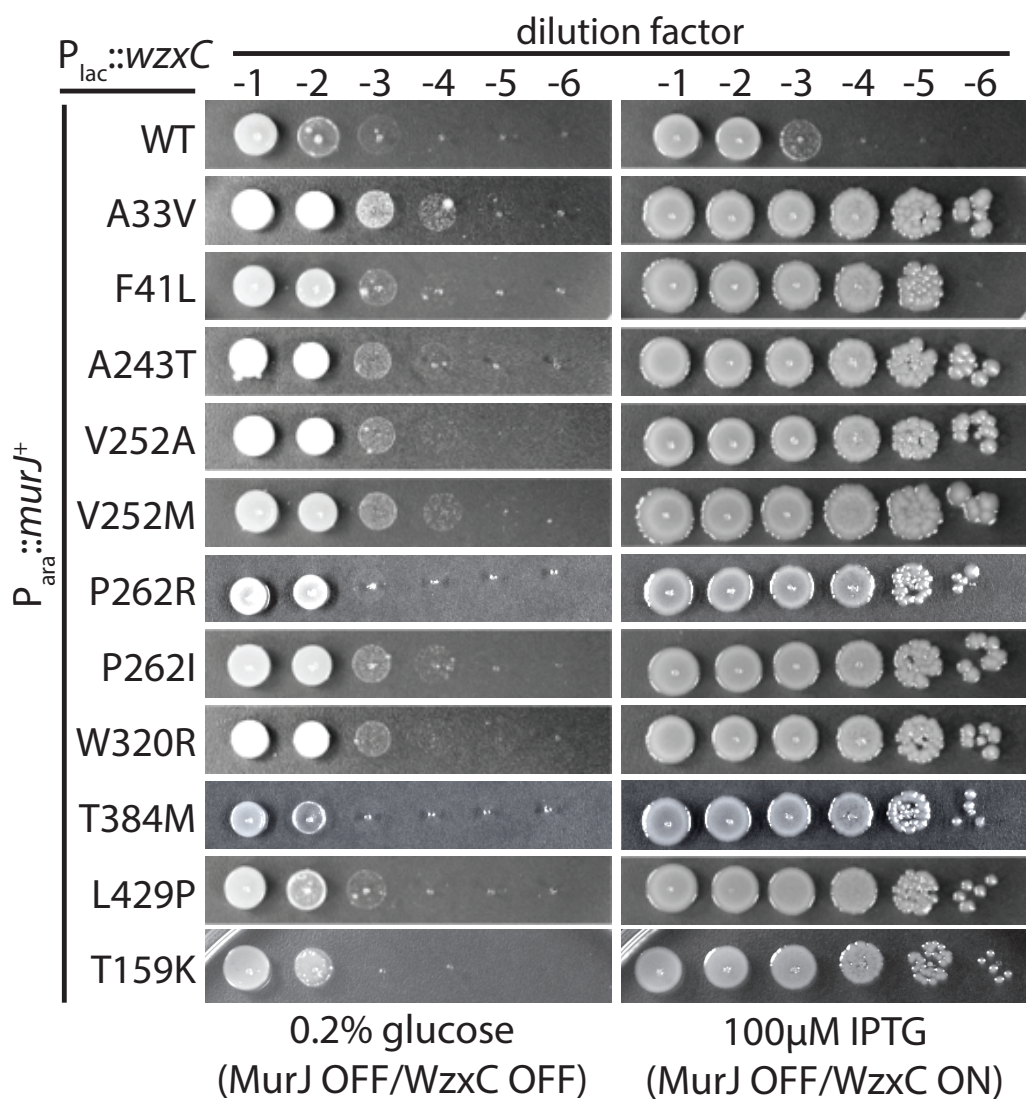


**Figure 1. WzxC variants can substitute for MurJ.** Cells of CS7 [ $P_{ara}::murJ$ ] harboring plasmids encoding C-terminally FLAG-tagged WzxC (WT) or the indicated derivatives were grown in LB medium with arabinose overnight. Following normalization for culture density, serial dilutions ( $10^{-1}$  to  $10^{-6}$ ) were prepared and  $5 \mu\text{l}$  of each were spotted onto LB plates supplemented with either glucose or IPTG. Plates were photographed after incubation at  $37^{\circ}\text{C}$  for  $\approx 16$  hours. All of the strains grew similarly on plates supplemented with arabinose under this condition. An additional growth experiment with additional concentrations of IPTG are presented in **SI Appendix, Fig. S2**.

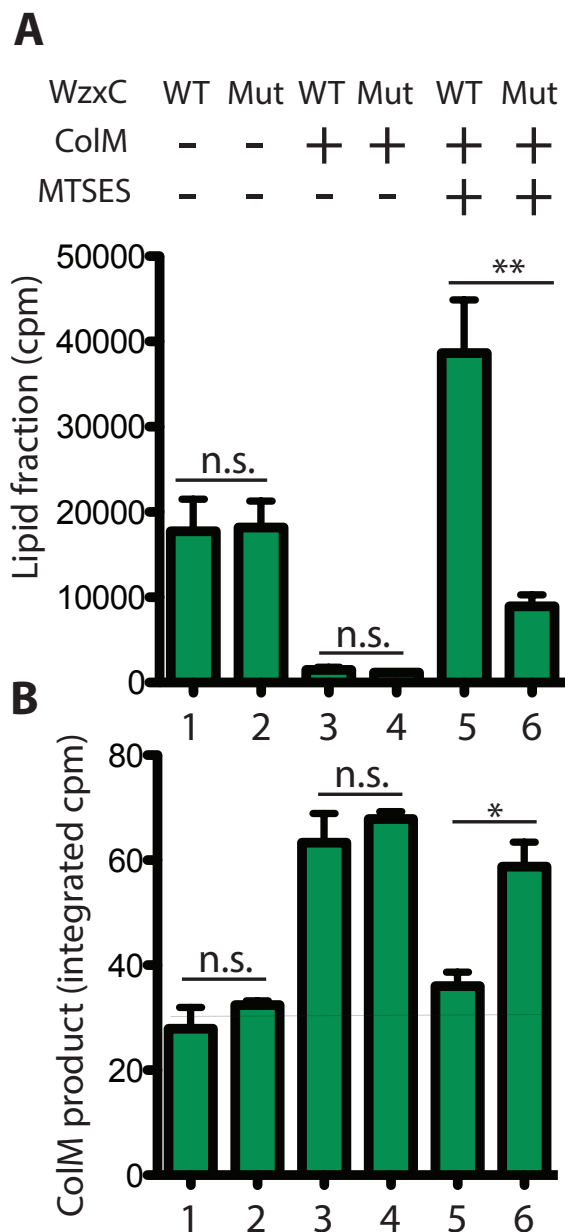


**Figure 2. Support of PG lipid-II flipping in vivo by a WzxC variant.** Cells of CAM290 [*murJ*(A29C)] harboring plasmid pCS124 [*P<sub>lac</sub>::wzxC*(WT)-*flag*] or pDF2 [*P<sub>lac</sub>::wzxC*(V252M)-*flag*] were grown in labeling medium to an OD<sub>600</sub> of 0.2. [<sup>3</sup>H]-mDAP was then added to radiolabel PG precursors. After a 15 min labeling period, MTSES and ColM were added to block MurJ(A29C) activity and cleave flipped lipid II, respectively. Just prior to cell lysis, cells were collected by centrifugation and fractionated to measure radioactivity in the PG lipid precursor pool (**A**) and soluble ColM cleavage product (**B**). WT and Mut denote WzxC(WT) and WzxC(V252M), respectively. The means and the standard error of means (SEMs) from three experiments are shown. P-values were calculated with two-tailed unpaired Student's t-test. \*,  $p < 0.05$ ; \*\*,  $p < 0.01$ ; n.s., not significant. cpm = counts per minute.

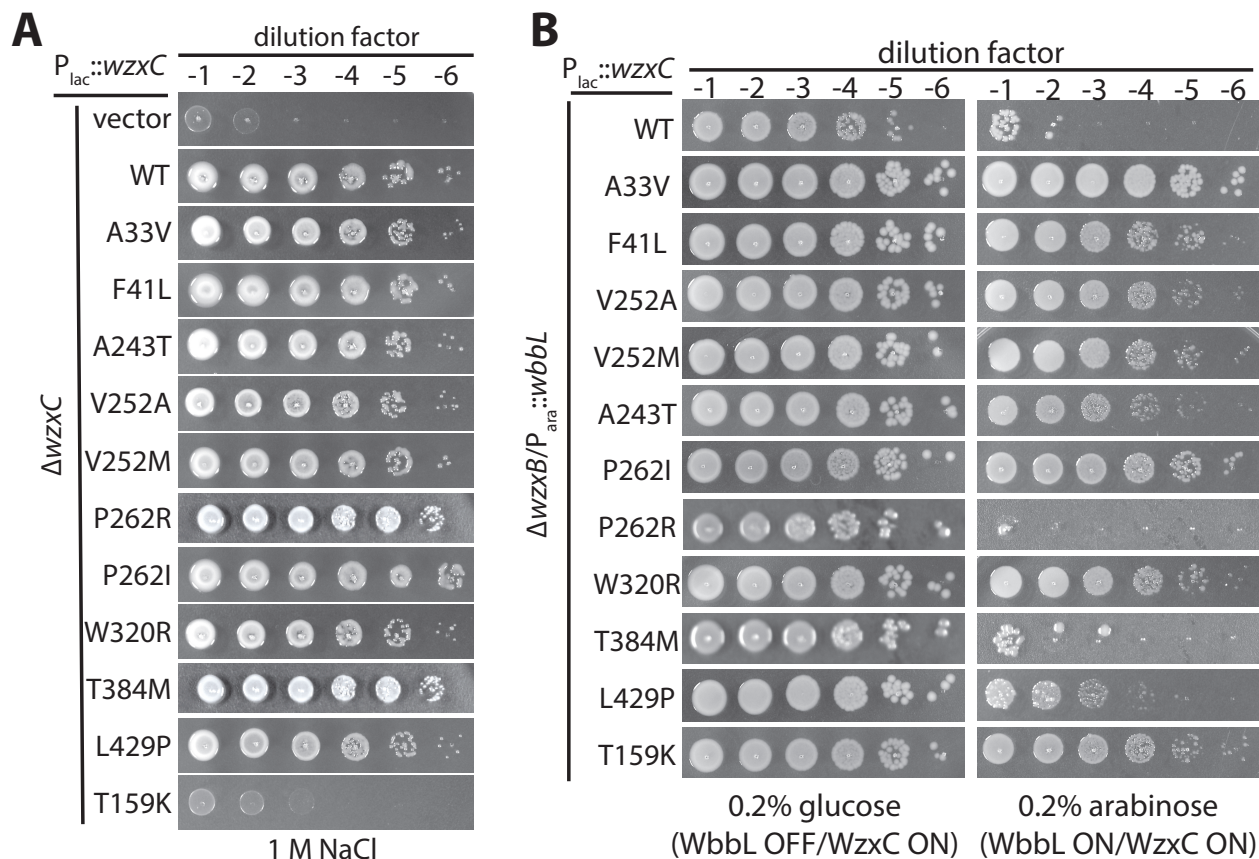


**Figure 3. Transport of colanic acid and O-antigen precursors by <sup>MJ</sup>WzxC variants.**

**(A)** Cells of CS38 [ $\Delta wzxC$ ] harboring an empty vector (vector) or vectors encoding the indicated FLAG-tagged WzxC variant were grown and plated on LB medium with 1M NaCl as described in Figure 1. Complementation of the  $\Delta wzxC$  phenotype results in the formation of mucoid colonies on the high-salt medium. **(B)** Cells of CS39/pCS160 [ $\Delta wzxB/P_{ara}::wbbL$ ] harboring the same WzxC-encoding plasmids were grown and diluted as described in Figure 1 followed by plating on LB medium with 100  $\mu$ M IPTG (to induce WzxC production) plus either glucose or arabinose (to repress or induce O-antigen production, respectively) as indicated.

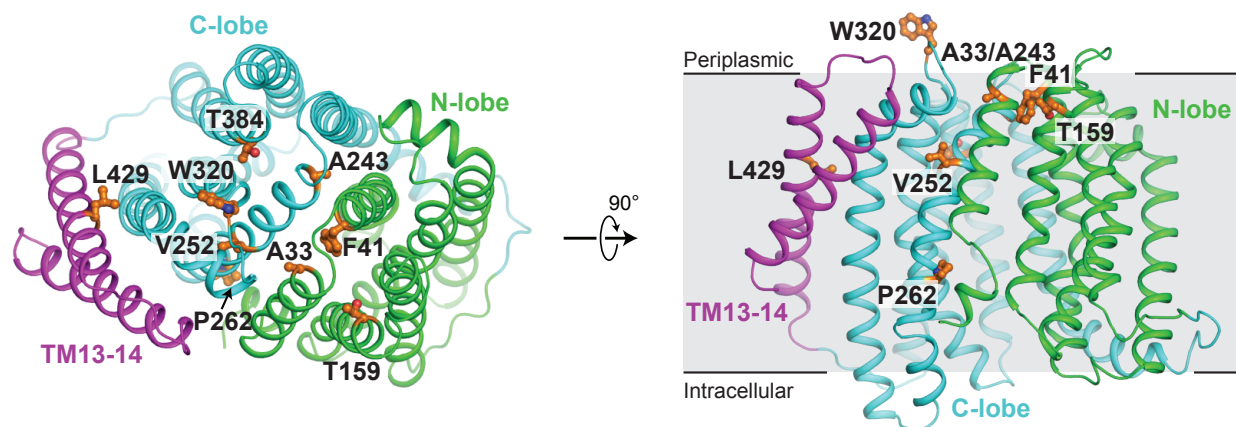


**Figure 4. Structural analysis of specificity-broadening mutations in WzxC.**

A homology model of WzxC is shown, with the sites of mutations highlighted in orange sticks. At left, the protein is viewed from the periplasmic side, and at right is viewed parallel to the membrane plane. With only a few exceptions, the mutations cluster at the periplasmic face of the protein near the interface between the N- and C-terminal lobes of WzxC.

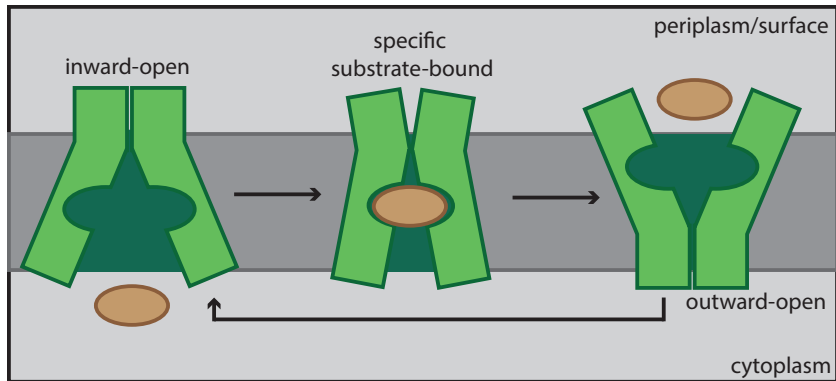


**Figure 5. Model for substrate induced conformational changes in MOP family flippases.** Shown is a schematic summarizing our model for substrate transport by MOP family flippases. Structural studies suggest that the inward-open conformation is the most stable state of the transporter. Based on our genetic results, we propose that specific substrate binding is required to break contacts at the outer face of the transporter to destabilize the inward-open conformation. Once these contacts are broken, a transition to the outward-open conformation can occur to allow for substrate release on the opposite face of the membrane. For simplicity, the lipid anchor of the substrate is not drawn.